NASA TECHNICAL MEMORANDUM

NASA TM X-52244

GPO PRICE $ _____

CFSTI PRICE(S) $ _____

Hard copy (HC) 1.00

Microfiche (MF) .50

ff 653 July 65

MIXING AND REACTION STUDIES OF HYDRAZINE AND NITROGEN TETROXIDE USING PHOTOGRAPHIC AND SPECTRAL TECHNIQUES

by Marshall C. Burrows
Lewis Research Center
Cleveland, Ohio

TECHNICAL PAPER proposed for presentation at Fifth Aerospace Sciences Meeting sponsored by the American Institute of Aeronautics and Astronautics
New York, New York, January 23-25, 1967

NATIONAL AERONAUTICS AND SPACE ADMINISTRATION · WASHINGTON, D.C. · 1966

MIXING AND REACTION STUDIES OF HYDRAZINE AND NITROGEN TETROXIDE USING PHOTOGRAPHIC AND SPECTRAL TECHNIQUES

by Marshall C. Burrows

Lewis Research Center
Cleveland, Ohio

TECHNICAL PAPER proposed for presentation at

Fifth Aerospace Sciences Meeting
sponsored by the American Institute of Aeronautics and Astronautics
New York, New York, January 23-25, 1967

NATIONAL AREONAUTICS AND SPACE ADMINISTRATION

MIXING AND REACTION STUDIES OF HYDRAZINE AND NITROGEN TETROXIDE USING PHOTOGRAPHIC AND SPECTRAL TECHNIQUES

by Marshall C. Burrows

Lewis Research Center
National Aeronautics and Space Administration
Cleveland, Ohio

Abstract

Distances required to atomize, mix, and react N_2H_4 and N_2O_4 were experimentally determined for a quadlet injector element at 19 atmospheres and an oxidant-fuel weight ratio of 1.0. Streams of like propellants were diagonally opposite at an impingement angle of 90°. Silhouette photographs showed that atomization of the propellant streams occurred in less than 1 inch, and vaporizing pockets of NO_2 extended downstream for 4 inches or less. Thermocouple measurements showed that the hottest gases were in the oxidant-rich zones; fuel-rich gases appeared to be influenced by the decomposition reaction of hydrazine. Temperatures approached steady-state values 11 inches or more from the injector. Spectral radiation bands of NH, OH, and NH_2 were most intense in the fuel-rich and well-mixed zones; pyrometer measurements of H_2O radiation were highest in the oxidizer-rich and well-mixed zones. Concentration profiles of H_2O were determined from measured radiation and gas temperature and plotted as a function of axial distance. The resulting curves compared favorably with H_2O concentrations calculated for combustion profiles limited by either fuel or oxidant vaporization.

Summary

Photographs, thermocouple measurements, and emission spectra were used to study the atomization, mixing, and reaction characteristics of hydrazine and nitrogen tetroxide. The propellants were injected through a quadlet element into a 2-inch diameter combustor at an oxidant-fuel weight ratio of 1.0, chamber pressure of approximately 19 atmospheres, and contraction ratio of 9.85. Propellant behavior was followed from the point of injection to the mixed product gases 18 inches downstream.

Silhouette photographs of the impinging jets indicated atomization of the liquid propellants occurred in less than 1 inch. Frame-by-frame study showed that perturbations in the atomization distance were repetitive with a period of approximately 0.8 milliseconds. Photographs taken through a transparent chamber showed that opaque pockets of NO_2 extended from 2 to 4 inches downstream from the injection point. Pockets of fuel-rich gases were essentially transparent and hence could not be distinguished downstream from the impingement point. When like propellants were injected on opposite sides of the element, the photographs showed that the fuel-injected sides of the chamber remained fuel-rich with respect to the metered oxidant-fuel weight ratio; oxidant-injected sides of the chamber remained relatively oxidant-rich. This behavior was attributed in part to interfacial or liquid phase reactions which were sufficiently fast and energetic to prevent appreciable jet interpenetration and mixing in the liquid phase.

Uncorrected measurements by tungsten-rhenium alloy thermocouples corresponded to maximum gas temperatures of 2910° K on the oxidizer-injected sides of the chamber, and 1750° K or more on the fuel-injected sides. The highest temperature, when corrected for losses, is close to the calculated stoichiometric gas temperature of 3160° K; the lowest temperatures are above the calculated temperature of 1465° K for hydrazine decomposing to ammonia, hydrogen, and nitrogen. Gas temperatures near the axis of the chamber indicated that products were well mixed at downstream axial distances of 11 inches or more from the injector.

Photographic emission spectra from the gases near the injector were limited principally to the transparent gases on the fuel-injected sides of the combustor. Spectral radiation from NH at 3360 Angstroms wavelength was concentrated close to the atomizing fuel jets and reached maximum intensity 1 inch from the impingement point of the jets. Intensities of the OH radical as measured by a photometer were consistently higher on the fuel-injected sides of the combustor in spite of higher measured gas temperatures on the oxidant-injected sides. At least part of this difference was attributed to the presence of NO and NO_2 on the oxidizer-injected sides. These gases absorb strongly in the ultraviolet range and therefore attenuate the OH radiation intensities for large distances downstream.

Total gas radiation, monitored by a pyrometer, was highest on the oxidizer-injected sides of the combustor for most of the chamber length. The near-infrared emission bands of water vapor were considered responsible for most of this radiation, and therefore the radiation intensity-distance curves were assumed to reflect the changes in water vapor concentration and temperature with mixing and reaction.

Measured gas temperatures and total radiation intensities were used with Planck's radiation law and a thin gas approximation (low gas emissivity) to calculate the concentration profiles of H_2O as a function of axial downstream distance. The resulting curves were compared with H_2O concentrations derived from combustion profiles limited by either fuel or oxidant vaporization. Comparison of curves showed that the experimentally determined concentrations matched those determined for vaporization-limited combustion if the fuel-rich and oxidant-rich sides of the chamber were considered.

It was concluded from this study that the impingement of hydrazine and nitrogen tetroxide in a quadlet element was not effective in producing a homogeneous mixture of fuel and oxidant, and that

the resulting stratification persisted for large axial lengths.

Introduction

Many researchers have considered the physical behavior of N_2H_4 and N_2O_4 jets to be approximately described by nonreactive and nonmiscible liquids (refs. 1 to 3). However, if the hypergolic properties of these propellants cause the jets to be diverted away from the impingement point, the propellants will not mix and react in the short distances necessary for good performance and hardware design, (refs. 4 to 6). Study of the physical behavior at the impingement point should therefore be coupled with examination of the corresponding chemical behavior in this region.

Analytical studies of hydrazine-nitrogen tetroxide performance have been hampered by a lack of information on the effects of atomization, vaporization, and the decomposition reactions of both propellants (refs. 7 and 8). Ignition and gas phase kinetic reactions have been studied for this system but corresponding studies in a high pressure combustor with liquid phase injection have been lacking (refs. 9 and 10).

It was the purpose of this study to obtain more information on the physical processes of atomization, vaporization, and mixing as well as determine by means of temperatures and emission spectra which controlling chemical processes are taking place. This information can serve to define a more accurate analytical model to the overall combustion of liquid hydrazine and liquid nitrogen tetroxide in a rocket combustion chamber.

Silhouette photographs were used to determine the chamber length required to atomize the impinging jets, vaporize and react the optically dense NO_2; and to observe time-varying processes near the impingement point. Tungsten/tungsten-rhenium thermocouples were used to determine the gas temperature profile as a function of axial downstream distance. Spectral radiation bands of NH, OH, and NH_2 were used to determine apparent decomposition and oxidation reaction zones. Pyrometer measurements of total radiation due primarily to H_2O radiation were used to determine the extent of reaction as a function of axial downstream distance. Experimentally determined H_2O concentrations were compared with those determined for vaporization-limited combustion.

Apparatus and Procedure

Combustor

An impinging quadlet injector element was used for all combustor tests. The four tubes were positioned as shown in figure 1, with impingement at an included angle of 90° (45° to the combustor axis). The inside diameter of each tube was 0.068±0.001 inch and the free stream length of each jet was less than 0.1 inch before impingement. The alignment of the tubes had a large effect on the axial symmetry of the spray pattern. Hence, the injector was inspected and flow checked with water periodically to insure constancy of test conditions.

All combustor parts except the nozzle were made of stainless steel to prevent surface reactions with the propellants and emission spectra from the metal oxides, especially copper. A copper nozzle was used since it maintained its dimensions better than stainless steel, and did not introduce any copper compound emission spectra. Run lengths were between 1.0 and 1.5 seconds, with equilibrium flow and chamber established 0.2 second or less after ignition. Chamber pressure was 19 atmospheres, oxidant-fuel weight ratio was 1.0 and contraction ratio was 9.85. At these conditions, the calculated jet velocity of the hydrazine was 95 feet per second and that of the nitrogen tetroxide was 64 feet per second. Windowed or transparent plastic chamber sections permitted observation of the combustor gases from the impingement point to 18 inches downstream.

Photographs

Illumination for silhouette photographs of the atomization zone was provided by a zirconium continuous arc source. Light passed through a converging lens, engine windows, and spray to the rotating prism camera. Effective exposure time for these photographs was 33 microseconds at a rate of 6000 frames per second per second. High speed tungsten rated color film was used in the camera.

Photographic spectra of the combustor gases were obtained on a 35 millimeter film strip using a 1.5 meter grating spectrograph with quartz optics. A spectral slitwidth of approximately 20 Angstroms was required for the 1.0 second exposure time. The shutter was programmed to open automatically in the middle of the combustor test run. The spectral range of the spectrograph was 2100 - 7800 Angstroms, but the spectral intensities within the combustor, and the photographic film limitations reduced this range to approximately 2500 to 6500 Angstroms.

Other Instrumentation

Ultraviolet radiation intensities in the spectral range 2600 - 4000 Angstroms were measured with a bandpass photometer consisting of an absorption filter, phototube with ultraviolet sensitivity, and amplifier. A voltage-time recorder plotted the average ultraviolet radiation intensity as a function of time. Total radiation intensities were recorded in the same manner, with a mirror-type pyrometer responding to infrared radiation between 0.8 and 3.5 microns.

Gas temperatures in the combustor were obtained from the thermovoltages generated by tungsten/tungsten-26 percent rhenium bare wire thermocouples. The junctions were welded beads approximately twice the 0.015 inch diameter of the wires. The junction extended approximately 0.1 inch from the alumina and stainless steel holder. Coating the metal with silicon rubber before each run increased the life of the alumina and stainless steel holder so that the thermocouples stayed in position long enough to reach equilibrium. Most of the thermocouple junctions withstood the combustion environment for at least one run, especially in the nonoxidizing (fuel-rich) gas zones. It is obvious that the oxidation of the junction itself could

increase the apparent temperature of the gases in oxidizer-rich zones. However, this will be most serious at mixture ratios greater than 1.5 and temperatures above 3000° K.

Readings were taken on opposite sides of the chamber, averaged if within 10 percent, or repeated if the difference was larger. The thermocouple measurements must be corrected for junction radiation and thermal conduction of the thermocouple wires. A maximum error in gas temperature of 300° K will occur at an indicated gas temperature of 2900° K if the combustor walls are assumed to be 1370° K, the gases within the chamber transparent, and the temperature of the thermocouple wire outside the combustor 300° K. The total error decreases to 20° K at an indicated temperature of 2260° K. Unfortunately, the exact error in temperatures caused by radiation and conduction of the thermocouple cannot be determined; the above assumptions were considered extreme.

Experimental Results

Silhouette Photographs

Photographs were taken with either the windowed or plastic chamber in position between the injector element and the nozzle, figure 2. They showed that the atomization distance was not constant, but varied from 0.3 to 1.3 inches from the impingement point, with an average distance of less than 1 inch. This variation was repetitive, with a period of approximately 0.8 millisecond. Injection velocities of the N_2H_4 and N_2O_4 were not equal (95 and 64 ft/sec); and axial velocities of the impinging liquids as measured from the photographs appeared to vary within those limits. Some photographs showed dense oxidizer streams returning to the combustor walls at an angle of 45° to the axis of the combustor. This behavior prevented complete mixing with or penetration of the fuel by the oxidizer streams. Performance tests at the Jet Propulsion Laboratory (ref. 6) using much larger unlike impinging jets indicated similar behavior. At a mixture ratio of 1.0, the momentum of the fuel streams exceeded that of the oxidizer streams by nearly 50 percent. Liquid fuel therefore tended to occupy the core of the impingement zone with the oxidizer streams repelled from the fuel at the interface.

Dense pockets of NO_2, identified by their reddish-brown color, extended downstream for approximately 4 inches with velocities that ranged from 65 to 190 feet per second, figure 3. Liquid N_2H_4, appearing as a gray area near the impingement point, disappeared soon after atomization was completed, e.g., 2 inches downstream.

Thermocouple Measurements

Gas temperatures within the combustor, as determined by tungsten/tungsten-26 percent rhenium thermocouples, varied from 1750° K on the fuel-injected sides of the combustor to 2910° K on the oxidant-injected sides of the combustor as shown in figure 4. Maximum combustor temperatures occurred on the oxidizer-injected sides from 2.75 to 5.5 inches from the impingement point. Temperatures on the fuel-injected sides were considerably lower; in the downstream positions, gases approached the temperatures of reacted and mixed products. The temperature profile across the chamber in the downstream positions was due to heat transfer to the combustor walls, radial variations in the oxidant-fuel weight ratio, or a combination of these factors. For example, a decrease in core temperature of 100° K, from 2760° K at 11 inches downstream to 2660° K at 18 inches downstream, can account for heat transfer to the walls of 1 Btu/(sq in.)(sec). As noted in figure 4, the gas temperatures derived from thermocouple measurements are uncorrected for radiation from the junction and conduction along the wires. Because of the low conductivity of tungsten, and the exposure of 0.1 inch of thermocouple wire to the high temperature gases, the major error in the thermocouple reading should be due to radiation losses from the junction. The estimated maximum temperature correction would raise the maximum measured gas temperatures from 2910° to 3210° K, or approximately 50° K above the calculated temperature for equilibrium products calculated according to the procedures outlined in reference 11.

Photographic Spectra

Spectra of the gases in the combustor were obtained for the ultraviolet and visible wavelength spectrum. OH bands from 2600 to 3500 Å and NH bands centered at 3360 and 3370 Å were the principal radiating species in the ultraviolet range. When either the photographic exposure or slitwidth was increased considerably, the NH_2 radiation bands from 5000 to 7000 Å were recorded. Ultraviolet and visible radiation from the combustor gases were considerably more intense on the fuel-rich sides of the combustor. For example, the NH band at 3360 Å reached a maximum intensity (corresponding to maximum density on the film) at a distance of 1 inch from the injector on the fuel-rich sides on the combustor as shown in figure 5. Oxidizer-rich gases apparently absorbed most of the NH radiation near the injector.

Photometer and Pyrometer Data

The ultraviolet OH bands and the infrared H_2O bands were considered the strongest spectral emitters in the combustor. A photometer and pyrometer, respectively, were the most reliable means of recording their radiant intensities in terms of average output voltages. Figure 6 shows the photometer output as a function of axial downstream distance from the injector. Ultraviolet emission from the gases increased in intensity with increasing axial distance, and was consistently higher on the fuel-rich sides of the combustor even though higher gas temperatures were recorded by the thermocouples in the oxidizer-rich gases. As in the case of NH, the OH radiation was attenuated by the oxidizer-rich gases.

Output of the total radiation pyrometer is shown in figure 7 as a function of the axial downstream distance for the fuel-injected and oxidizer-injected sides of the combustor. Infrared intensities increased rapidly for the first 4 inches from the injector and then slowly increased to final values that were close to the mixed equilibrium-product radiation. Total radiation from gases on the oxidizer-injected sides was

consistently higher than that on the fuel-injected sides for most of the combustor length. This result is in contrast to that for the ultraviolet radiation which was higher on the fuel-injected sides of the combustor.

Occasional combustor tests showed an oscillatory rather than stable pressure environment with an amplitude as high as 50 percent of the chamber pressure. The mode of oscillation was identified as the first longitudinal mode. Generally, mixing was enhanced by the oscillatory burning, and the radiation intensities on the fuel-injected sides of the combustor became equal to those on the oxidizer-injected sides. This is shown in figure 6 for ultraviolet radiation as well as in figure 7 for the infrared radiation data.

Discussion

Large density and temperature gradients within the combustor reduced the spatial resolution of the photographs in figure 2, and the 33 microsecond exposure time of each frame was too long to stop high-velocity droplets. However, the photographs did show the approximate end of propellant ligaments from 0.3 to 1.3 inches from the impingement point. Any liquid that extended beyond this distance should be in the form of individual droplets.

Based on the variation in injection velocities of the propellants, the average 1-inch atomization distance corresponds to a time of 0.9 to 1.3 milliseconds. It is perhaps fortuitous that these times bracket the minimum ignition delay observed for these propellants in the liquid phase in bomb tests of 1.2 milliseconds, reference 12. Aside from this comparison, there did not appear to be any large, highly exothermic reaction upon impact of the fuel and oxidizer streams. Thermocouples placed at or slightly below the impingement point remained essentially at liquid temperature. The only indication of immediate reaction between the fuel and oxidizer was a repelling force encountered at the impingement point. The jets, rather than forming a uniform propellant distribution, appeared to be repelled after contact and, returned to the sides of the chamber from which they were injected.

It was estimated that the heat released by the interfacial reaction between hydrazine and nitrogen tetroxide was 0.015 percent of the total energy available (data obtained from B.P. Breen of Dynamic Science Corporation, Monrovia, California). Even this small quantity of heat was considered sufficient to overcome the momentum of impingement and keep the oxidizer and fuel separated. That study considered the unlike impingement of N_2H_4 and N_2O_4 at an angle of 90°. In this study, with like propellant tubes opposed as shown in figure 1(c), the contact area between unlike propellants would not be a plane surface, but rather an irregular surface which is a function of the momentum ratio between the two propellants. A few combustor tests were made with like propellants in adjacent tubes as in figure 1(d). Combustor performance decreased considerably, and photographs showed even more stratification of the propellants as they moved down the chamber on the same sides that they were injected. It was obvious that the injector arrangement of figure 1(c), provides better distribution of the propellant streams.

A large number of possible reactions are available in the hydrazine-nitrogen tetroxide system. Ignition kinetics have been investigated by Skinner et al. (ref. 9), and the steady state behavior was studied in a reactor by Sawyer (ref. 10). In both studies, the decomposition of hydrazine formed an essential part of the overall reaction mechanism. The simple reaction, $N_2H_4 \rightarrow N_2 + 2H_2$ is not followed but rather the more exothermic one: $2N_2H_4 \rightarrow 2NH_3 + N_2 + H_2$. Decomposition of liquid hydrazine at 298° K therefore results in an equilibrium gas temperature of 1465° K for a heat of reaction of 23.1 kcal/mole of hydrazine. The lowest gas temperature measured in the combustor was 1750° K at 2.75 inches from the injector, which may correspond to fuel decomposition in that region. This was confirmed by a spectrogram of the emitting gases which showed NH and NH_2 radical emission in the fuel-rich zones immediately downstream of the injection point. These radicals are considered an initial product of the overall N_2H_4 decomposition, reference 13. Maximum NH radiation at 1 inch from the fuel side of the injector therefore indicates maximum decomposition of the hydrazine at the same point that atomization takes place.

The oxidation reactions in the combustor were coincident with or closely followed the decomposition of the fuel, since OH radiation was always observed in regions that strongly emitted NH_2 and NH. This observation is consistent with the proposed reaction mechanisms of Sawyer, reference 10, in which an initial step in the reaction of N_2H_4 and N_2O_4 is the formation of NO and OH. N_2H_4 reacts further with NO and OH to form the final products N_2 and H_2O. In terms of the overall reaction mechanism, the suggested oxidation reactions are:

$$N_2H_4 + NO_2 \rightarrow \frac{1}{2} N_2H_4 + H_2O + NO + \frac{1}{2} N_2 \qquad (1)$$

$$\frac{1}{2} N_2H_4 + NO \rightarrow H_2O + N_2 \qquad (2)$$

$$N_2H_4 + NO_2 \rightarrow 2H_2O + \frac{3}{2} N_2 \qquad (3)$$

No emission bands due to NO were observed in the emission spectra from the combustor. Since their wavelengths are close to those for OH, weak emission bands could be masked by the very intense OH bands, reference 14.

Assuming that the water vapor in the combustor always remains in thermal equilibrium, and that its emission band account for most of the infrared radiation, its concentration can be determined as a function of the axial distance downstream from the injector. The fuel-rich and oxidant-rich sides of the combustor must be considered separately because of the marked differences in measured radiation and temperature profiles. The equilibrium concentration of H_2O can be calculated from the equation:

$$\frac{P_{H_2O}}{P_o} = \frac{\lambda^5 T_G}{KLP_oT_oC_1} \left(e^{C_2/\lambda T_G} - 1 \right) \qquad (4)$$

where

P_{H_2O} is the partial pressure of water vapor in atmospheres

K is a constant which includes the integrated absorption coefficient

L is the optical path length through the combustor, assumed constant at 5 cm

P_o, T_o are the reference pressure and temperature of 19 atm and 2600° K, respectively

C_1, C_2 are constants in Planck's Radiation law

λ is the effective wavelength of water vapor radiation, assumed equal to 2.6 microns

T_G is the gas temperature, taken as the average of the two thermocouple radial locations, and corrected for the maximum radiation loss.

The mole fraction of water vapor is assumed equal to 0.4 at 18 inches downstream, the value calculated from equilibrium products at a fuel-oxidant weight ratio of 1.0 from reference 11. This equation is valid for gases with a low emissivity, that is, "thin gas approximation."

Concentration profiles of the water vapor were plotted as a function of axial downstream distance in figure 8. On the fuel-rich sides of the combustor, the maximum mole fraction of H_2O occurred from 2 to 3 inches downstream. This maximum results from the relatively high measured radiation at these positions coupled with corresponding low gas temperatures. It is possible that radiation from the 2.2 micron band of NH_3 may become important near the injector. In that case, the maximum would represent an effect of the hydrazine decomposition reaction as well as those reactions producing H_2O. On the oxidant-injected sides of the combustor, the mole fraction of H_2O increased continuously with increasing distance.

If the extent of reaction within the combustor can be assumed to be primarily controlled by vaporization of one or both propellants, a profile of H_2O concentration as a function of axial downstream distance similar to experimentally derived curves can be computed. The combustion reaction, if limited by the vaporization of fuel, will proceed at an initially high oxidant-fuel weight ratio. The reverse will be true of oxidant-limited vaporization. Because of the observed stratification of the propellant mixture, the oxidant-injected sides of the combustor were assumed to be limited in oxidant vaporization with an overall mixture ratio greater than 1.0; gases on the fuel-injected sides were assumed to be limited in fuel vaporization with an overall mixture ratio less than 1.0. Details of the calculation are given in the appendix. Curves showing the best fit to the data are plotted in figure 8. Mole fractions derived from the two sources agree well considering the assumptions that were necessary. Satisfactory data on turbulent mixing are not available for this system, and a comprehensive model including both vaporization and mixing effects could not be used.

Conclusions

The results of this study show that the impingement of hydrazine and nitrogen tetroxide resulted in rapid atomization of the liquid jets, but did not produce a homogeneous mixture of fuel and oxidant droplets within the chamber. Homogeneous product gases were obtained only by mixing lengths greater than 18 inches or by the mixing achieved by longitudinal pressure oscillations.

Gas temperatures derived from uncorrected thermocouple measurements varied from 300° K above the fuel decomposition temperature on the fuel-sides of the combustor to 250° K below the stoichiometric product temperature on the oxidant-injected sides of the combustor. Relatively constant thermal profiles were established at 11 inches or more from the injector.

Spectral radiation intensities of NH, OH, and H_2O were determined as a function of axial downstream distance from the injector. Gas temperatures and radiation intensities due to H_2O were used with Planck's law and a thin gas approximation to calculate the concentration profiles of H_2O as a function of axial downstream distance. The resulting curves compared favorably with H_2O concentrations derived from the extent of combustion as limited by either fuel or oxidant vaporization.

Appendix

Calculated water vapor concentrations were derived from combustion profiles based on the vaporization rate of either the fuel or oxidizer. The percentages of vaporized propellants in the combustor can be related to the combustion efficiency η by the equation, reference 7:

$$\eta = \frac{\left(c^*_{th}\right)_{\mathcal{O}/\mathcal{F}}}{\left(c^*_{th}\right)_{o/f}} \left(\frac{\mathcal{O}\dot{w}_o + \mathcal{F}\dot{w}_f}{\dot{w}_o + \dot{w}_f} \right)$$

where o/f is the metered oxidant-to-fuel weight ratio, $\dot{w}_o/\dot{w}_f$.

$\mathcal{O}/\mathcal{F}$ is the ratio of vaporized oxidant to vaporized fuel, $\mathcal{O}\dot{w}_o/\mathcal{F}\dot{w}_f$

$\mathcal{O}$ is the percentage of vaporized oxidant

$\mathcal{F}$ is the percentage of vaporized fuel

$\dot{w}_o$ is the liquid oxidant weight flow, lb/sec

$\dot{w}_f$ is the liquid fuel weight flow, lb/sec

With the oxidant vaporization limiting the rate of reaction, the combustion efficiency can be written:

$$\eta = \frac{\left(c^*_{th}\right)_{\mathcal{O}/f}}{\left(c^*_{th}\right)_{o/f}} \frac{\frac{\mathcal{O}\dot{w}_o}{\dot{w}_f} + 1}{\frac{\dot{w}_o}{\dot{w}_f} + 1}$$

- If the fuel limits the rate of reaction, the efficiency is:

$$\eta = \frac{\left(c^*_{th}\right)_{o/\mathcal{F}} \frac{\dot{w}_o}{\dot{w}_f} + \mathcal{F}}{\left(c^*_{th}\right)_{o/f} \frac{\dot{w}_o}{\dot{w}_f} + 1}$$

The variation of theoretical c^* over a range of mixture ratios was calculated for equilibrium gaseous products at a chamber pressure of 20 atmospheres, reference 11. Then using the above equations, c^* efficiency η was plotted as a function of the percentage of propellant vaporized, as shown in figure A-1. Reference 7 also presents a correlation of the generalized chamber length as a function of propellant vaporized. Within the combustor, chamber length can be written in the form:

$$l_c = l_{gen}\left(\mathcal{A}^{0.44}\right)\left(1 - T_{l,o,R}\right)^{0.4} \times \left(\frac{\mathcal{M}_m}{0.003}\right)^{1.45} \left(\frac{v_o}{1200}\right)^{0.75} \times \left(\frac{\lambda}{140}\right)^{0.8} \left(\frac{\mathcal{M}_a}{100}\right)^{0.35} \left(\frac{P_c}{300}\right)^{-0.66}$$

which for a chamber pressure P_c of 20 atmospheres and median drop size of 0.003 inches reduces to:

$$l_c = l_{gen}\left(\mathcal{A}^{0.44}\right)\left(1 - T_{l,o,R}\right)^{0.4} \times \left(\frac{v_o}{1200}\right)^{0.75} \left(\frac{\lambda}{140}\right)^{0.8} \left(\frac{\mathcal{M}_a}{100}\right)^{0.35}$$

where l_{gen} is the generalized length parameter

$T_{l,o,R}$ is the ratio of propellant temperature to its critical temperature

v_o is the injection velocity, in./sec

λ is the latent heat of vaporization, Btu/lb

$\mathcal{M}_a$ is the molecular weight of propellant, lb mass/lb mole

$\mathcal{A}$ is the contraction ratio of the combustor

For hydrazine, the variation in chamber length with the generalized length parameter becomes $l_c = l_{gen}(0.65)$, and for nitrogen tetroxide, $l_c = l_{gen}(1.14)$. The correlation curve in figure 28(f) of reference 7 can be used with the above expressions to obtain the variation in chamber length as a function of the vaporized mass of propellant, as shown in figure A-2. Since the oxidant vaporization curve is above that of the hydrazine, it is apparent that the combustion in the chamber is limited by the oxidant vaporization to a greater extent than by fuel vaporization for a given chamber length.

The vaporized propellant can be related to the extent of combustion by calculating the apparent local oxidant-to-fuel weight ratio as a function of downstream position. If equilibrium products are assumed at each position, a water vapor concentration can be calculated for each local mixture ratio. Figure A-3 shows various H_2O concentration profiles as a function of axial distance for a metered oxidant/fuel weight ratio of 1.0. Stratified mixture ratios on the oxidant-injected sides and the fuel-injected sides of the combustor were 2.0 and 0.5; 1.5 and 0.67; and 1.25 and 0.8, respectively.

References

1. Rupe, J. H., "The liquid-phase mixing of a pair of impinging streams," Jet Propulsion Lab., California Institute of Technology PR 20-195 (August 6, 1953).

2. Rupe, J. H., "A correlation between the dynamic properties of a pair of impinging streams and the uniformity of mixture-ratio distribution in the resulting spray," Jet Propulsion Lab., California Institute of Technology PR 20-209 (March 28, 1956).

3. Rupe, J. H., "An experimental correlation of the nonreactive properties of injection schemes and combustion effects in a liquid-propellant rocket engine. Part I: The application of nonreactive-spray properties to rocket-motor injector design," Jet Propulsion Lab., California Institute of Technology TR 32-255, NASA CR-64635 (July 15, 1956).

4. Stanford, H. B., and Tyler, W. H., "Injector development," Jet Propulsion Lab., California Institute of Technology Space Programs Summary No. 37-31, Volume IV, NASA CR-62607 (February 28, 1965).

5. Elverum, G. W., Jr., and Staudhammer, P., "The effect of rapid liquid-phase reactions on injector design and combustion in rocket motors," Jet Propulsion Lab., California Institute of Technology PR 30-4 (August 25, 1959).

6. Johnson, B. H., "An experimental investigation of the effects of combustion on the mixing of highly reactive liquid propellants," Jet Propulsion Lab., California Institute of Technology TR 32-689, NASA CR-64616 (July 15, 1965).

7. Priem, R. J. and Heidmann, M. F., "Propellant vaporization as a design criterion for rocket-engine combustion chambers," NASA TR R-67 (1960).

8. Beltran, M. R., and Rosvic, T. C., "Parametric study of combustion instability in MMH-NTO liquid rocket engine," AIAA Paper 66-603, 1966.

9. Skinner, G. B., Hedley, W. H., and Snyder, A. D., "Mechanism and chemical inhibition of the hydrazine-nitrogen tetroxide reaction," Monsanto Research Corp., AFASD-TDR-62-1041 (December 1962).

10. Sawyer, R. F., "The homogeneous gas phase kinetics of reactions in the hydrazine-nitrogen tetroxide propellant system," Princeton University TR 761, AFOSR-66-0855, AD-634277 (1965).

11. Zeleznik, F. J. and Gordon, S., "A general IBM 704 or 7090 computer program for computation of chemical equilibrium compositions, rocket performance, and Chapman-Jouguct detonations," NASA TN D-1454 (October 1962).

12. Weiss, H. G., Johnson, B., Fisher, H. D., and Gerstein, M., "Modification of the hydrazine-nitrogen tetroxide ignition delay," AIAA J. 2, 2222-2223 (1964).

13. Eberstein, I. J. and Glassman, I., "The gas-phase decomposition of hydrazine and its methyl derivatives," Tenth International Symposium on Combustion (Combustion Institute, Pittsburgh, 1965) p. 365.

14. Pearse, R. W. B. and Gaydon, A. G., The Identification of Molecular Spectra (Chapman and Hall, Ltd., London, 1963) 3rd ed.

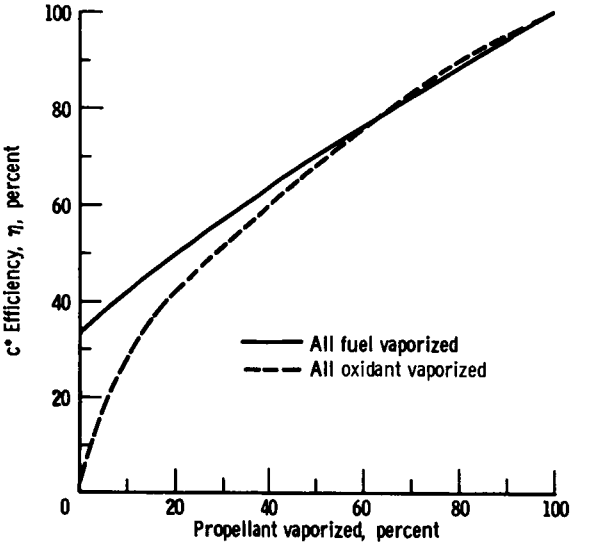

Figure A-1. - Vaporization-limited combustion efficiency; O/F = 1.0, N_2H_4 - N_2O_4 (ref. 7).

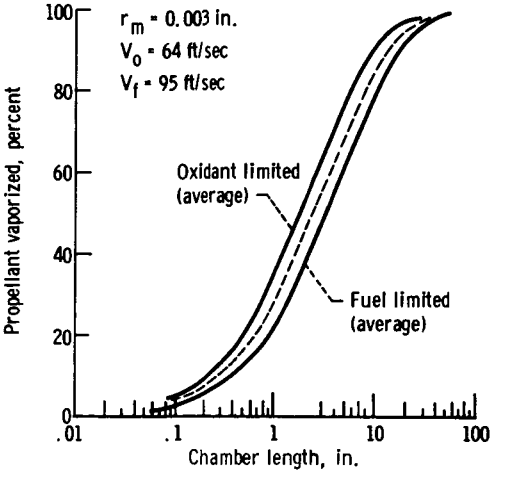

Figure A-2. - Vaporization-limited combustion, N_2H_4 - N_2O_4.

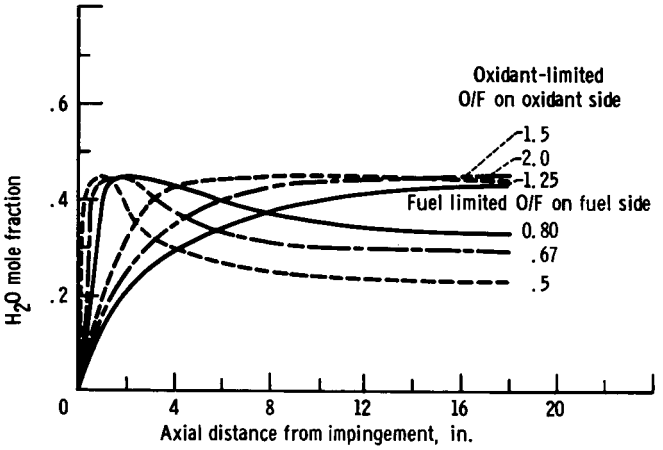

Figure A-3. - Calculated H_2O concentration profiles in combustor. Metered O/F = 1.0; P_c = 19 atmospheres.

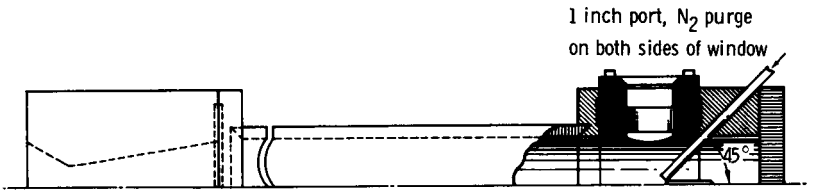

(a) Combustor with stainless steel windowed chamber.

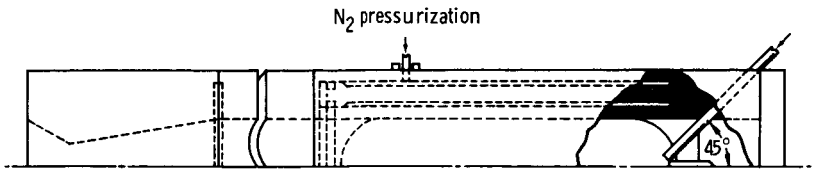

(b) Combustor with 8 inch cast acrylic chamber.

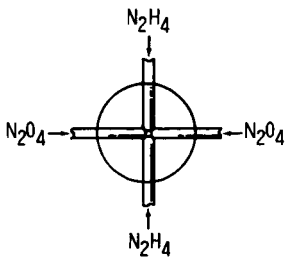

(c) like-on-like impingement.

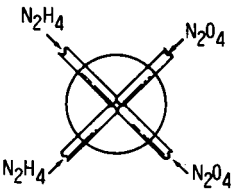

(d) Unlike impingement.

Figure 1. - N_2H_4 - N_2O_4 combustor. Injector: 4-0.068 in. i.d. tubes at 45° to combustor axis. Chamber: 2 in. diameter, 20 inches long. Nozzle: 0.640 in. diameter, 3 in. conical convergence.

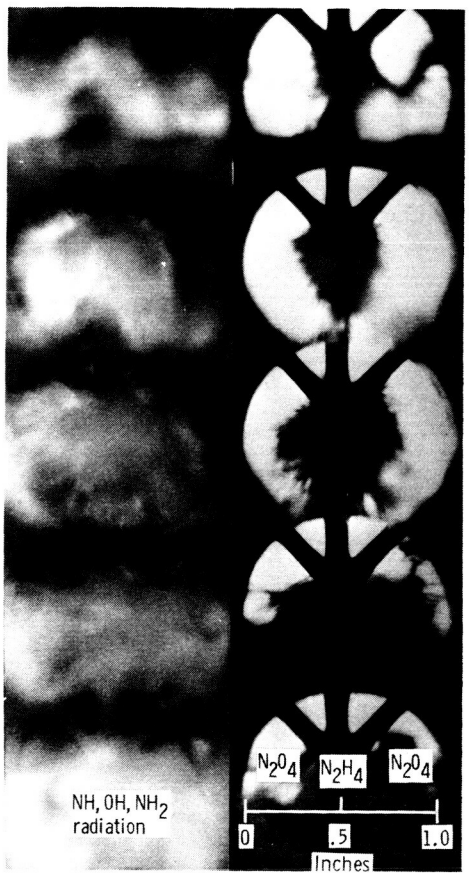

(a) Blue exposure due to OH and NH gas radiation.

(b) Red exposure of liquid jets silhouetted by zirconium arc.

Figure 2. - Photographs of impinging N_2H_4 and N_2O_4 in windowed chamber. Fuel jets, front and rear; oxidant jets right and left. 6000 frames/sec; exposure 33×10^{-6} sec at F/2.8. Prints derived from 16 mm. color transparencies.

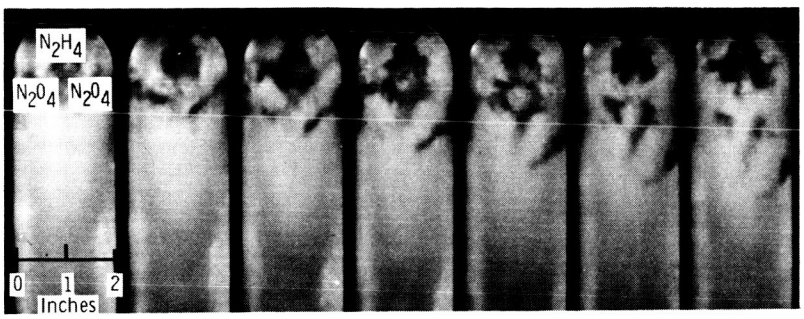

(a) Fuel jets front and rear; oxidant jets right and left.

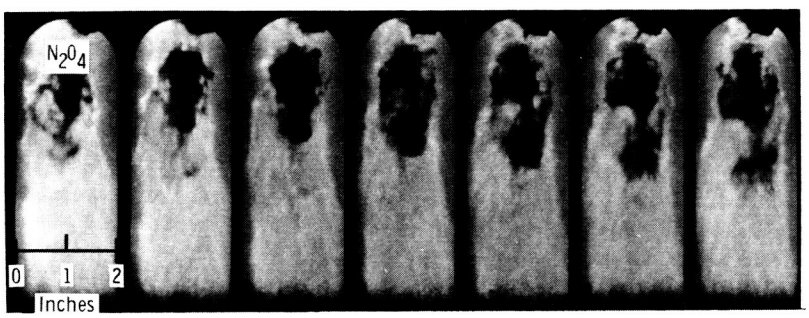

(b) Fuel jets right and left, oxidant jets front and rear. 6000 frames/sec; exposure 33×10^{-6} sec at F/2.8.

Figure 3. - Photographs of impinging jets of N_2H_4 and N_2O_4 in transparent chamber.

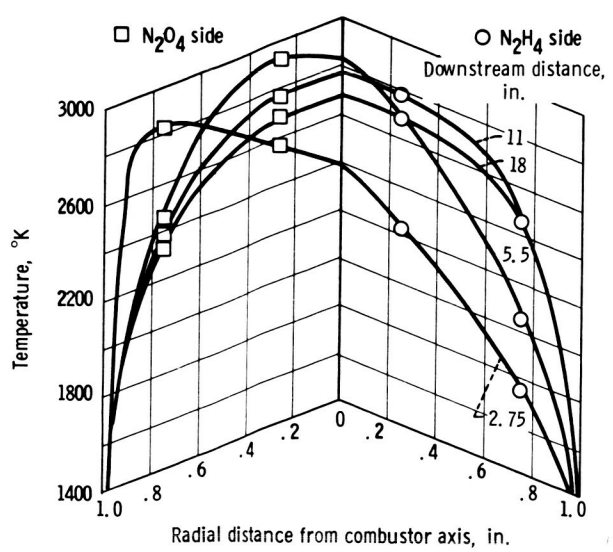

Figure 4. - Uncorrected gas temperature profile at various distances from the injector; O/F = 1.0.

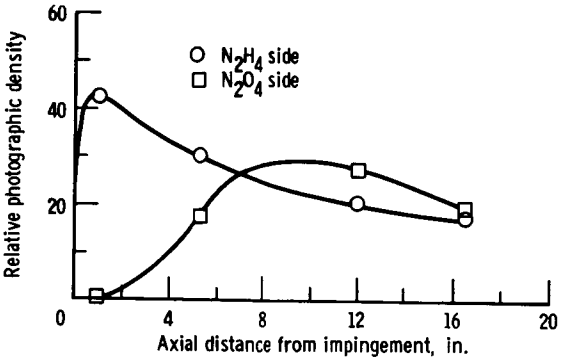

Figure 5. - 3360 Å NH spectral band density as a function of axial distance; O/F = 1.0; P_c = 19 atmospheres.

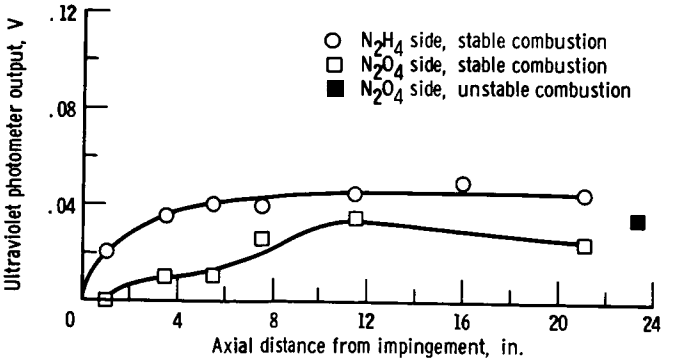

Figure 6. - uv radiation as function of axial distance. Principal emitter, OH, 2600 - 4000 Å; O/F = 1.0; P_c = 19 atmospheres.

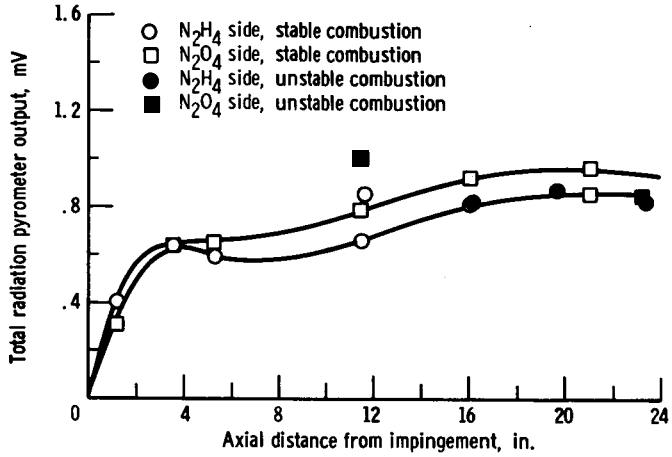

Figure 7. - Total radiation as function of axial distance. Principal emitter, H_2O bands at 0.9, 1.1, 1.4, 1.9, 2.7 microns; O/F = 1.0; P_c = 19 atmospheres.

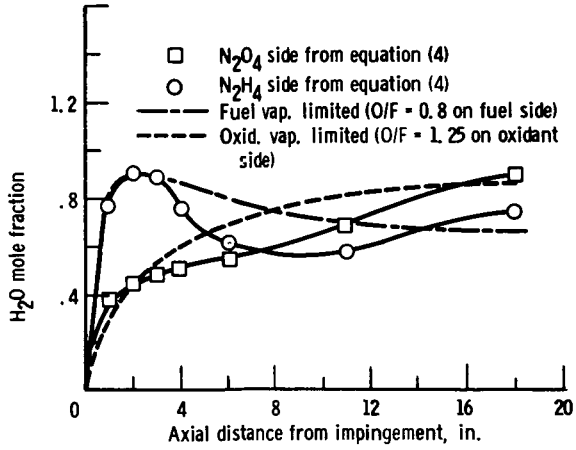

Figure 8. - Comparison of H_2O concentration profiles in combustor. Metered O/F = 1.0; P_c = 19 atmospheres.